The contribution of active and passive mechanisms of 5mC and 5hmC removal in human T lymphocytes is differentiation- and activation-dependent

Lucia Vincenzetti[1], Cristina Leoni[1], Michele Chirichella[1], Ivo Kwee[1] and Silvia Monticelli[1]*

[1] Institute for Research in Biomedicine (IRB), Università della Svizzera italiana (USI), Via Vincenzo Vela 6, CH-6500, Bellinzona, Switzerland

* Corresponding author (silvia.monticelli@irb.usi.ch)

Keywords

DNA methylation, epigenetics, T lymphocytes, differentiation, activation

Abstract

In mammals, the 5'-methylcytosine (5mC) modification in the genomic DNA contributes to the dynamic control of gene expression. 5mC erasure is required for the activation of developmental programs and occurs either by passive dilution through DNA replication, or by enzymatic oxidation of the methyl mark to 5-hydroxymethylcytosine (5hmC), which can persist as such or undergo further oxidation and enzymatic removal. The relative contribution of each mechanism to epigenetic control in dynamic biological systems still remains a compelling question. To explore this critical issue, we used primary human T lymphocytes, in which two cellular states can be clearly identified, namely quiescent naïve T cells, which are slowly or rarely proliferating, and rapidly proliferating activated T cells. We found that active mechanisms of methylation removal were selectively at work in naïve T cells, while memory T lymphocytes entirely relied on passive, replication-dependent dilution, suggesting that proliferative capacity influences the choice of the preferential demethylation mechanism. Active processes of demethylation appear to be critical in quiescent naïve T lymphocytes for the maintenance of regulatory regions poised for rapid responses to physiological stimuli.

Introduction

The methylation of the cytosine base (5mC) in the genomic DNA is essential for mammalian development and for cell lineage specification, and is intimately linked with the regulation of gene expression [1]. The bulk genomic methylation patterns are mostly static in differentiated cells and tissues, with large stably methylated regions including the inactive X chromosome, imprinted genes, pericentromeric repeats and other repeated elements, and transposable elements [2]. Despite its stability and heritability across cell division, dynamic changes in 5mC deposition are observed during development and differentiation, and are deemed to be necessary for the establishment of stable cell-specific gene expression programs [3]. Once deposited in the genome, 5mC can be removed either through passive dilution during DNA replication, which occurs if the methyl mark is not copied on the nascent DNA strand, or through active mechanisms mediated by enzymes of the TET (Ten-eleven translocation) family (TET1-3). The 5mC mark is oxidized by TET proteins to 5-hydroxymethylcytosine (5hmC), which can then undergo further oxidation processes [4, 5]. 5hmC is however a stable mark that can accumulate to significant levels (up to 0.6% of total nucleotides in post-mitotic Purkinje neurons [6]), contributing to the regulation of gene expression, possibly by recruiting readers of this modification [3]. Differently from 5mC, 5hmC is enriched within the gene bodies of highly transcribed genes and at functional regulatory elements such as enhancers [3, 7-9], while the vast majority of repetitive elements is enriched with 5mC but not 5hmC [9]. The 5hmC modification can therefore act both as an intermediate of active DNA demethylation and as a stable epigenetic mark [3, 10].

Whereas basic mechanistic aspects of passive and active DNA demethylation are well characterized, it is still unclear what is their relative contribution to the dynamic removal of 5mC and 5hmC in evolving biological systems. Therefore, we set out to address this critical issue in a cellular system, human T helper (T_H) lymphocytes, in which antigen-induced differentiation and activation is associated with extensive functional reprogramming and persistent changes in cellular physiology. Following the first recognition of a foreign infectious agent, antigen-inexperienced naïve T_H cells undergo rapid proliferation, and at the same time differentiate into an array of memory and effector subsets, with responses tailored towards the specific pathogen being recognized [11]. At a molecular level, T cell activation and acquisition of effector functions occur through the combinatorial action of transcription factors and epigenetic mechanisms to finally establish transcriptomes distinctive of each subset [12]. 5mC and 5hmC have a variable impact on T cell phenotypes, as inferred by mouse models lacking either DNMT or TET enzymes. For example, DNA methylation and DNMT enzymes were shown to influence the expression of the *Il2*, *Il4* and *Ifng* cytokine genes in both $CD4^+$ and $CD8^+$ mouse T cells [13-19]. Genome-wide studies of DNA methylation also highlighted the extent of changes accompanying the acquisition of the effector/ memory phenotype upon stimulation of mouse and human naïve T cells [20-23], with progressive demethylation correlating with differentiation of memory cells. Finally, DNA methylation changes and histone modifications occurring during cell cycle progression were shown to control T cell differentiation in the mouse [24]. As for 5hmC, it is enriched inside the body of highly expressed genes in murine T lymphocytes and at active thymus-specific enhancers, suggesting a possible role during T cell development and differentiation [7]. However, germline deletion of mouse *Tet2* led to largely normal B and T lymphocyte development [8, 25], although *Tet2* deletion in early lymphoid progenitors determined a partial reduction of IFN-γ and

IL-17 expression by the T_H1 and T_H17 lymphocyte subsets, respectively [26]. In humans, T cell activation was associated with an incompletely characterized global reduction in genomic 5hmC, as well as with a modest gain of 5hmC at specific genomic regions associated with T cell activation [27].

Our data now indicate that naïve T cells rely significantly on an active process of 5hmC removal, while active removal of modified cytosines could not be detected in memory lymphocytes, which instead used passive, replication-dependent dilution of the modified cytosines. Our data point to the notion that the preferential usage of active *vs*. passive mechanisms of DNA demethylation is differentiation- and activation stage-dependent, with active demethylation mechanisms being selectively involved in quiescent naïve T cells to maintain regulatory regions poised for rapid responses to stimuli.

Results

DNA methylation and hydroxymethylation dynamics upon T cell activation. We first determined the global changes of genomic 5mC and 5hmC upon activation of primary human T lymphocytes. Naïve (T_N) and memory (T_{MEM}) cells were separated from the peripheral blood of healthy donors and were either left unstimulated or stimulated for 5 days with anti-CD3 and anti-CD28 antibodies. Levels of genomic 5mC and 5hmC were then determined by dot blot. Consistent with a role for DNA demethylation specifically during cell differentiation, there was a trend (although not statistically significant), towards slightly higher levels of 5mC in naïve compared to memory T cells (**Figure 1a-b**) [21]. Accordingly, in naïve cells, levels of 5mC were modestly reduced after 5 days of activation, while memory T cells showed negligible changes upon acute stimulation. Compared to 5mC, the dynamic range of changes in genomic 5hmC appeared to be much greater, with a global reduction that affected more than 87% of the initial 5hmC levels in recently activated naïve cells (**Figure 1c**). The overall levels of 5hmC were significantly higher (~4.6-fold) in resting naïve compared to resting memory or activated T cells, effectively separating naïve T cells from all antigen-experienced T lymphocytes (**Figure 1c-d** and **Suppl. Figure 1**). Such difference was not justified by the observed differences in 5mC: when calculating the ratio between 5hmC and 5mC, unstimulated naive cells maintained levels of 5hmC that were ~4.3-fold higher compared to those of all other T cell subsets (**Figure 1e-f** and **Suppl. Figure 1**).

The mammalian genome is heavily and stably methylated, especially at stably heterochromatic regions such as centromeric repeats, transposons and the inactive X chromosome [2], making bulk changes in 5mC difficult to detect, as they are restricted to a much smaller fraction of the genome (active genes and enhancers) than that associated with constitutive methylation. Therefore, on a global scale, changes in 5hmC provide a more sensitive, albeit indirect, readout of the dynamic changes in methylation occurring at gene bodies and regulatory regions [9]. Indeed, loss of 5hmC indicates either its passive dilution or the further oxidation followed by base excision and replacement with an unmethylated cytosine. We therefore analyzed changes in levels of genomic 5hmC in various conditions of T cell activation. First, similarly to $CD4^+$ T cells, a robust difference between naïve and memory cells was observed in human $CD8^+$ T cells, which displayed a strong reduction in 5hmC upon activation (**Figure 2a**). The same phenomenon was also observed in mouse $CD4^+$ and $CD8^+$ T cells activated *in vitro* with anti-CD3 and anti-CD28 antibodies for 3 days (**Figure 2b-c**). The high levels of genomic 5hmC characteristic of naïve T cells are likely to ensue during thymocyte development in the transition between the double-positive (DP) and single-positive (SP) stage (**Suppl. Figure 2**), although in peripheral cells they may also derive from ongoing processes of 5mC oxidation.

Within the human memory compartment, effector memory T lymphocytes (T_{EM}) showed the lowest 5hmC content, while central memory T cells (T_{CM}) showed intermediate levels between naive and T_{EM} cells (**Figure 2d**), suggesting that low levels of 5hmC correlate with differentiation of T cells towards an effector phenotype. Different effector subsets, such as T_H1, T_H2 and T_H17 showed low levels of 5hmC that were comparable to those of T_{EM} cells (less than 1 pmol/ μg of genomic DNA) (**Figure 2e**), indicating that the global 5hmC reduction is a general feature of T cell activation and differentiation and is not subset-specific.

DNA demethylation favors the acquisition of an effector T cell phenotype. Having established that levels of 5hmC (and to a lesser extent 5mC) are globally reduced upon activation and differentiation of naïve T cells, we then asked whether the link between DNA demethylation (of which 5hmC represents an intermediate) and acquisition of effector functions might be causal. First, we found that the treatment of naïve and memory human T lymphocytes with decitabine (DAC), an inhibitor of DNA methyltransferases, led to a modest (not statistically significant) reduction in global 5mC in proliferating cells (**Figure 3a-b**). The observed effect on a global genomic scale was mild, since this method is insufficiently sensitive to detect changes in DNA methylation at specific, immune-relevant genes. Notwithstanding this technical limitation, treatment with DAC led to the acquisition of a more effector-like phenotype by naïve cells upon stimulation, suggesting that levels of DNA methylation impact differentiation of naive T cells, resulting in a significant increase in the expression of IFN-γ and IL-22 to levels that were fully comparable to those of memory T cells, along with a modest reduction in IL-2 expression (**Figure 3c** and **Suppl. Figure 3**). Such effect was less apparent in differentiated memory T cells that are already capable of optimal cytokine expression.

To further clarify the role of DNA demethylation in regulating the acquisition of an effector phenotype in T cells, we enhanced TET activity by either over-expressing TET proteins (**Figure 3d-e**) or by vitamin C treatment (**Figure 3f-g** and **Suppl. Figure 4**). Our initial experiments showed that transfection or transduction of proteins as large as the TET enzymes in primary T cells was sufficient to affect T cell activation and even more proliferation, resulting in confounding consequences on the final biological effects. We therefore transfected the full-length TET proteins in Jurkat T cells, whose proliferation was instead unaffected. The three TET enzymes were variably effective at increasing the levels of genomic 5hmC in these cells, with TET2 and TET1 being the most and the least effective, respectively (**Figure 3d**). Despite its low efficacy in this system, TET1 was expressed by transfected Jurkat cells as expected, it was able to re-activate expression of fully methylated, non-replicable reporter plasmids, and it was functional in immunofluorescence experiments using 5hmC as readout (**Suppl. Figure 5**). However, TET1 was shown to be unable to induce global DNA demethylation, but instead to counteract the spreading of DNA methylation at regulatory regions, potentially explaining its limited efficacy in our system [28]. Notwithstanding such differences among TET proteins, increased levels of 5hmC invariably correlated with a modest increase in cytokine expression by Jurkat cells, suggesting that enhancing levels of genomic 5hmC in already differentiated cells only modestly increased transcription of genes already amenable of expression (**Figure 3e**). A catalytically inactive version of TET2 (H1302Y and D1304A) [29, 30] was unable to increase either 5hmC levels or cytokine expression (**Figure 3d-e**), suggesting that the observed effects were indeed dependent on the catalytic activity of TET enzymes, although the effect on cytokine transcription could be direct or indirect.

To determine the effect on T cell differentiation, which cannot be assessed in Jurkat cells, we used vitamin C treatment to enhance the general activity of all TET enzymes in primary T cells. Vitamin C was shown to act as a co-factor to maintain the essential atom of iron in the catalytic site in a reduced state [30-32], and to influence differentiation of regulatory T cells in both human and mouse, enhancing their suppressive capacity [33]. Treatment of activated naïve and memory T lymphocytes with increasing concentrations of vitamin C led to a corresponding increase in the global 5hmC levels, as assessed by dot blot (**Figure 3f**). Increased 5hmC levels correlated with a significantly increased,

albeit modest in magnitude, capacity of memory, but not naïve T cells to produce cytokines, as determined by intracellular staining (**Figure 3g** and **Suppl. Figure 4**). These findings suggest that while DNA demethylation events (as in the DAC-treated cells) favor the differentiation of T cells into an effector phenotype, enhancing the activity of TET enzymes is instead insufficient to significantly alter the differentiation of naïve T lymphocytes, although it can induce a modest increase in gene expression at loci that are already accessible for transcription in differentiated memory T or Jurkat cells.

Changes in 5hmC do not require TCR engagement and are predominantly linked to T cell proliferation. We dissected the relative roles of T cell activation and proliferation in the global changes of 5hmC observed upon stimulation of T lymphocytes. To assess whether T cell receptor (TCR) signaling was required for such changes in 5hmC, freshly isolated $CD4^+$ naive, T_{CM} and T_{EM} cells were cultured in the presence of IL-2, IL-6 and TNF-α to induce cytokine-driven proliferation [34, 35] in the absence of TCR engagement. The extent of cell proliferation in each of the subsets (as measured by CFSE dilution) reflected their activation requirements, as naive cells could barely proliferate in the absence of full antigenic stimulation, while T_{EM} cells proliferated efficiently and T_{CM} cells displayed an intermediate phenotype (**Figure 4a**). In each case, the bulk levels of genomic 5hmC inversely correlated with the extent of T cell proliferation (**Figure 4b-c**). A similar result was observed in primary human $CD8^+$ T cells undergoing homeostatic proliferation upon culture with IL-7 and IL-15 [36] (**Figure 4d-e**), suggesting that T cell proliferation, rather than TCR-dependent activation, is the main driver of the observed reduction in genomic 5hmC.

To further determine whether the reduction in 5hmC that was observed upon T cell proliferation was exclusively linked to passive dilution, we optimized systems to uncouple T cell activation from proliferation. First, we defined the changes in levels of genomic 5hmC at early time points of T cell activation, prior to cell cycle progression. After stimulation with plate-bound anti-CD3 and anti-CD28 antibodies, we monitored T cell activation by measuring the surface induction of the early activation markers CD25 and CD69 (**Figure 5a**). After 30 h of activation, cells were uniformly $CD69^+$ (which is an earlier marker of activation compared to CD25) and 40-60% of them were already also $CD25^+$, indicating effective activation. However, 30 h of stimulation were insufficient for cells to engage in cell division, which occurred only after 48 h (**Figure 5b**). In these experimental conditions, we found that 5hmC levels remained stable in the initial stages of activation (until 24 h after activation), and decreased rapidly and significantly (by about half) as soon as naïve and memory T cells entered cell division (48 h time point); however, we detected a modest but significant decrease in 5hmC in naïve, but not memory T cells prior to cell cycle progression, indicating that an active removal of 5hmC may be at play specifically in naive T lymphocytes (**Figure 5c-d**). To further explore this issue, naïve and memory T lymphocytes were loaded with CFSE and were then stimulated with plate-bound anti-CD3 and anti-CD28 antibodies. After 3 days, cells underwent about three cycles of cell division (**Figure 5e**). To address whether levels of 5hmC diminished with each cycle, we separated cells contained in each CFSE peak by sorting and we measured the global levels of 5hmC by dot blot. We found that memory T cells showed no detectable sign of active 5hmC removal, as the levels of 5hmC dropped exactly by half within the first cycle and then became somewhat stabilized at very low levels (**Figure 5e**). Naïve T cells showed instead a reduction in 5hmC levels at the first cycle that was higher than

expected, pointing once again towards a combination of active and passive mechanisms of removal of this modified base specifically in these cells.

To clarify whether indeed an active process of removal of 5hmC may be operating in naïve T cells, we stimulated naïve and memory T lymphocytes in the presence or absence of the cell cycle inhibitors nocodazole or aphidicolin. Nocodazole interferes with microtubule polymerization, including the mitotic spindle, thereby blocking the cells in the G2/M phase, while aphidicolin is a reversible inhibitor of the DNA polymerase α resulting in a block in the G1/S phase. After 3 days, untreated cells underwent at least three division cycles, while treated cells were for the most part blocked, as determined by CFSE dilution (**Figure 6a**). Despite the block in proliferation, T cells were effectively activated, as shown by the induced expression of CD25 (**Figure 6a**). In memory T cells, inhibition of the cell cycle almost completely counteracted the reduction in genomic 5hmC observed in untreated cells (**Figure 6b-c**), pointing towards a passive, proliferation-dependent mechanism of dilution of 5hmC in activated memory T lymphocytes. Conversely, treated naïve T lymphocytes showed a significant loss of genomic 5hmC upon activation, even in the complete absence of proliferation (**Figure 6b-c**). Overall, our data point towards the existence of active mechanisms of removal that are operating specifically in naïve T cells prior to cell-cycle entry, while memory T lymphocytes rely primarily on mechanisms of proliferation-dependent dilution.

Changes in 5hmC at enhancer regions distinguish early and late response genes. We further investigated changes in 5mC and 5hmC both genome-wide and at specific loci relevant for T cell functions. First, we performed reduced representation bisulfite sequencing (RRBS) to generate genome-scale DNA methylation profiles. This method directly measures the cytosine methylation state at high CpG-density sequences such as promoters and a subset of repetitive sequences [37, 38]. We found that the majority of differentially methylated regions were observed comparing naïve to memory T cells, consistent with previous studies [21, 22], while fewer differences were observed upon short-term activation of memory and naïve T lymphocytes (**Figure 7a** and **Suppl. Figure 6**). The observed differentially methylated regions were primarily located within introns and intergenic regions, although hypermethylation at some promoter regions was acquired by memory T cells, as compared to naïve cells, regardless of short-term stimulation (**Figure 7a** and **Suppl. Figure 6**), possibly contributing to T cell differentiation. Indeed, analysis of the gene ontology (GO) terms [39] associated with the differentially methylated promoter regions (defined as -1500bp from the transcription start site (TSS) of the closest gene) identified categories reflecting the underlying T cell biology (**Figure 7b**). For instance, hypo-methylated regions were associated with NF-kB signaling and positive regulation of cytokine and chemokine secretion, while hyper-methylated regions were primarily associated to regulation of transcription, but also to regulation of TCR signaling and of memory T cell differentiation.

Because 5hmC is usually enriched at regulatory regions such as enhancers [7, 9], to assess whether changes in 5hmC could more specifically distinguish patterns of gene expression in human T lymphocytes, we analyzed available hMeDIP-seq (hydroxymethylated DNA immunoprecipitation and sequencing) data [27] performed on primary human naïve T cells and *in vitro* differentiated T_H1 and T_H2 subsets. We focused our analysis on two categories of genes, namely *i)* genes induced in the absence of cell division (including early genes, activated within a few hours after T cell activation,

such as *IL2RA*), and *ii)* late genes, such as *IFNG*, that require multiple cell divisions and DNA demethylation-linked processes before being effectively transcribed [40]. At the interrogated regulatory regions of early response genes (*IL2RA*, *CD69*, *ICOS* and *LTA*), we found high levels of 5hmC in resting cells, followed by a general reduction consistent with the global decrease in 5hmC observed in activated, proliferating cells (**Figure 7c** and **Suppl. Figure 7a**). As observed by Nestor and colleagues [27], we were not able to identify any specific immunologically relevant gene in which a significant loss of 5hmC occurred between day 0 and day 1 of activation. The observed active loss of 5hmC is therefore likely to be due to a global remodeling, not selectively impacting one or few genes. Late genes (*IFNG*, *IL4*, *CD70*, *GZMB* and *CXCL10*) showed instead comparatively low basal levels of 5hmC in their regulatory regions at resting state, followed by an increase during differentiation and proliferation, suggesting a role for 5hmC in facilitating transcription of these genes in differentiated T lymphocytes (**Figure 7c** and **Suppl. Figure 8**). Interestingly, housekeeping genes (genes whose expression did not change in the different conditions analyzed) showed either no change of 5hmC (e.g. *SDHA*) or followed the general reduction in 5hmC observed after activation and proliferation (**Figure 7c** and **Suppl. Figure 7b**).

We then confirmed changes in 5mC and 5hmC at the regulatory regions of specific immunologically relevant genes by methylated and hydroxymethylated DNA immunoprecipitation (MeDIP and hMeDIP) followed by qPCR. We selected *IL2* and *IL2RA* as early genes and *IFNG* as a late gene. We observed a variable and generally very modest, if any, reduction in the levels of 5mC at the *IL2* and *IL2RA* enhancers (**Figure 7d**, top). Consistent with previous studies demonstrating a strong correlation between hypomethylation of the proximal *Infg* enhancer and expression of IFN-γ in mouse T_H1 cells [41], we found that this regulatory region, corresponding to the mouse CNS-6 (conserved non-coding sequence at -6 kb) was methylated in resting human naïve T cells, and underwent demethylation upon activation (**Figure 7d**, top). As for levels of 5hmC, the *IL2* and *IL2RA* enhancers showed a general 5hmC reduction following activation, consistent with the global loss of genomic 5hmC observed after cell activation and proliferation, while the *IFNG* proximal enhancer region showed a significant 5hmC increase, mirroring the changes in 5mC at this region (**Figure 7d**, bottom). Changes in 5hmC were therefore more dynamic than those in 5mC and appeared to have a distinct behavior in early (5hmC reduction) and late (5hmC increase) response genes, at least at the interrogated regulatory sequences for selected immune-relevant genes. Whether these may represent more general trends in other biological systems or conditions remains to be determined.

High levels of 5hmC may be critical especially in non-proliferating cells to maintain regulatory regions in an accessible state, amenable of transcriptional activation even in quiescent cells. To explore this possibility, we analyzed available ATAC-seq (Assay for Transposase-Accessible Chromatin and sequencing) datasets in human naïve T cells [42]. Our analysis revealed that ATAC-accessible regions were indeed enriched of 5hmC (**Figure 7e**). Overall, our data are consistent with a model in which in the absence of cell proliferation, 5hmC enables the expression of housekeeping and early response genes, presumably by counteracting DNA methylation at these regions. Conversely, a small subset of effector genes acquired 5hmC upon activation and proliferation, and these changes correlated with gene expression.

Discussion

Cell cycle progression is a key mechanism to relieve epigenetic repression during development and differentiation, while terminally differentiated cells acquire a relatively more stable epigenetic landscape. Our data now show that active removal of cytosine modifications contributes significantly to the first activation of naïve T lymphocytes, while replication-dependent dilution is the driving force leading to 5hmC reduction in highly proliferative already differentiated cells.

If 5hmC is diluted predominantly through DNA replication, why is it important for T cells in the first place? One possibility is that the activity of TET proteins is required to counteract the 'spreading' of DNA methylation to regions that are not actively transcribed in resting lymphocytes, but require fast activation upon antigen recognition. Indeed, we found that regulatory regions of early response genes, namely genes that can be rapidly transcribed upon activation of resting cells and in the absence of proliferation, were characterized by the presence of 5hmC, suggesting that 5hmC-dependent processes may be required to counteract deleterious methylation at these regions. The 5hmC modification at such early response genes was then lost by passive dilution, once the cells overcame their activation threshold and entered the cell cycle. Housekeeping genes, that require expression even in the absence of proliferation, showed either no changes in 5hmC levels or a reduction correlating with the general loss of 5hmC observed in proliferating cells. Finally, activation of late effector genes correlated with an increase of 5hmC at their regulatory regions, likely to be associated with active transcription and the necessity to establish a stably permissive chromatin landscape at these enhancers in differentiated cells. The fact that DNA methylation has the tendency to accumulate to transcriptional inactive genes [2], and at enhancers that are not actively bound by transcription factors (a process that would be extremely deleterious for genes encoding for effector cytokines) was already proposed with the discovery that DNA-binding factors were necessary and sufficient to induce local demethylation, and that loss of transcription factor binding was conversely sufficient for DNA methylation [43, 44]. This is also in line with recent findings showing that the activity of TET proteins is important to safeguard promoters from *de novo* methylation in embryonic stem cells (ESCs), thereby preserving appropriate lineage-specific transcription upon differentiation [45, 46]. Similarly, TET1 was shown to prevent the spreading of DNA methylation at CpG islands [28], and also to be required in germ cells to provide efficient protection from aberrant DNA methylation, thereby stabilizing the acquired epigenetic landscape after reprogramming events [47].

In T lymphocytes, the primary role of 5hmC would therefore be to counteract DNA methylation especially in resting, non-proliferating naïve T cells, which cannot exploit passive, cell cycle-dependent mechanisms of dilution as a 'resetting' device of wrongful methylation. Such mechanism may be especially important for human naïve T lymphocytes: differently from the mouse, in which the average lifespan of a naïve T lymphocyte is only 6-10 weeks, individual human naïve T cells can persist for 5-10 years without losing significant functionality [48-52]. Similarly to human naïve T cells, 5hmC-mediated processes may be crucial in rarely dividing or post-mitotic cells, such as neurons, in which replication-dependent dilution cannot occur, and that indeed present exceptionally high levels of 5hmC in their genome [6]. During mouse brain development, 5hmC was shown to be present at poised (yet dormant) loci, in order to facilitate activation at later developmental stages [53].

A second related possibility is that the presence of 5hmC may be required at specific enhancers to somehow create a 'window of opportunity' for enhancer demethylation upon T cell activation, which

is no longer required once the cells are appropriately activated and can enter proliferation. Indeed, a model in which 5hmC could be part of enhancer activation processes somewhat independently of 5mC was already proposed [44], in which 5hmC may counteract gene silencing by opposing chromatin states that would impede transcription, for example through the specific recruitment of yet to be identified effector molecules.

Once T lymphocytes become activated and enter a differentiation pathway towards effector cells, they become 'locked' in a less plastic memory/ effector state in which demethylation-dependent mechanisms are likely to become progressively relatively less relevant. Indeed, many mechanisms contribute to the maintenance of the differentiated state, including histone modifications at lineage-specific enhancer genes and specific expression of master transcription factors essential for lineage determination [11, 54, 55]. For example, permissive histone modifications can be observed at the murine *Ifng* locus early after T cell activation in both T_H1 and T_H2 polarizing conditions, but a T_H1-specific pattern becomes apparent as early as 48 hours after stimulation [56]. However, stable commitment to a single lineage was shown to require three-to-four cycles of cell division [40]; once this threshold was passed, polarized lymphocytes maintained expression of their specific lineage-appropriate cytokines even upon removal of polarizing stimuli. The fact that DNA-demethylation processes may become less relevant as cell differentiation progresses can be also inferred by the fact that enhanced TET activity in already activated memory T lymphocytes or in Jurkat cells revealed only a modest effect on gene expression.

Altogether, our data corroborate a model in which 5hmC may be required to maintain enhancer accessibility in resting T lymphocytes, thereby counteracting DNA methylation of essential regions that must retain a poised state for rapid responses upon encounter with an antigen.

Material and Methods

Primary human T cell isolation and culture. Blood from healthy donors was obtained from the Swiss Blood Donation Center of Basel and Lugano (Switzerland), with informed consent from the Swiss Red Cross and authorization number CE 3428 from the Comitato Etico Canton Ticino. Mononuclear cells were separated from peripheral blood using Ficoll-Paque Plus (GE Healthcare). $CD4^+$ or $CD8^+$ T lymphocytes were further isolated by positive selection using magnetic microbeads (Miltenyi Biotec). Naive and memory T cell subsets were then sorted based on the expression of the following surface markers: naïve $CD4^+$ T cells: $CD4^+CD25^-CD45RA^+CCR7^+$; memory $CD4^+$ T cells: $CD4^+CD25^-CD45RA^-CCR7^{+/-}$; T_H1 cells: $CD4^+CD25^-CD45RA^-CCR6^-CXCR3^+$; T_H2 cells: $CD4^+CD25^-CD45RA^-CCR6^-CCR4^+$; T_H17 cells: $CD4^+CD25^-CD45RA^-CCR6^+CCR4^+$, T_{CM} (central memory): $CD4^+CD25^-CD45RA^-CCR7^+$; T_{EM} (effector memory): $CD4^+CD25^-CD45RA^-CCR7^-$; naïve $CD8^+$ T cells: $CD4^-CD45RA^+CCR7^+$; memory $CD8^+$ T cells: $CD4^-CD45RA^{+/-}CCR7^{+/-}$. Cells were sorted using a FACSAria III (BD Biosciences) and the gating used for sorting are shown in **Suppl. Figure 9**. Human T cells were cultured in RPMI-1640 medium supplemented with 1% glutamine, 1% non-essential amino acids, 1% sodium pyruvate, penicillin, streptomycin, 50 µM β-mercaptoethanol and 5% human serum. For *in vitro* stimulation, T lymphocytes were stimulated using plate-bound anti-CD3 (clone TR66; 5 µg/ml) and anti-CD28 (1 µg/ml) antibodies. All flow cytometry and cell-sorting experiments adhered to recommended guidelines [57]

T cell proliferation and treatments. To measure proliferation, human T lymphocytes were labeled with carboxyfluorescein succinimidyl ester (CFSE, 5 µM, Thermo Fischer Scientific) for 8 min at 37°C, followed by extensive washing. For experiments of *cytokine-induced proliferation*, different subsets of $CD4^+$ T lymphocytes were cultured for 6 days in 96-flat bottom microplates in the presence of recombinant IL-2 (300 U/ml), IL-6 (25 ng/ml) and TNF-α (25 ng/ml). $CD8^+$ naïve and memory T cells were cultured in the presence of IL-7 (25 ng/ml) and IL-15 (25 ng/ml). All recombinant cytokines were purchased from Peprotech. For *demethylation experiments*, $CD4^+$ naïve and memory T cells were activated for 5 days in the presence or absence of decitabine (5-aza-2'-deoxycytidine, Sigma-Aldrich) used at 1 µM and 5 µM, or were pre-treated for 48h with vitamin C (50 and 100 µg/ml, Sigma-Aldrich), prior to activation. For experiments using *cell cycle inhibitors*, $CD4^+$ naïve and total memory T cells were activated for 3 days in the presence of aphidicolin (1 µg/ml, Sigma-Aldrich) or nocodazole (2 µg/ml, Sigma-Aldrich). All flow cytometry and cell-sorting experiments adhered to recommended guidelines [57]

Mouse T cell isolation and culture. Spleens were obtained from 8 weeks-old C57BL/6 male mice and homogenized to single cell suspensions. T cells were isolated by negative selection ($CD19^-$ $CD11c^-CD11b^-$). $CD4^+$ or $CD8^+$ naïve T cells were then sorted based on the following markers: naïve $CD4^+$: $CD3^+CD4^+CD8\alpha^-CD62L^{high}CD44^{low}$; naïve $CD8^+$: $CD3^+CD4^-CD8\alpha^+CD62L^{high}CD44^{low}$. Murine T cells were cultured in RPMI-1640 medium supplemented with 1% glutamine, 1% non-essential amino acids, 1% sodium pyruvate, penicillin, streptomycin, 50 µM β-mercaptoethanol and 10% fetal bovine serum (FBS). T lymphocytes were activated with plate-bound anti-CD3 (BioLegend, clone 145_2c11; 2 µg/ml) and anti-CD28 (BioLegend, clone 37.51; 2 µg/ml) antibodies, with addition of 100 U/mL of recombinant IL-2 (Peprotech) after the first 48 hours of stimulation. Animal studies were performed in accordance with Swiss Federal Veterinary Office guidelines and approved by the

Cantonal animal experimentation committee, Dipartimento della Sanità e della Socialità Canton Ticino (authorization TI 17-2013).

Surface and intracellular stainings. To assess the expression of surface markers of early T cell activation, cells were stained with anti-CD25 (Beckman Coulter) and anti-CD69 (BioLegend) antibodies conjugated to different fluorochromes. To measure cytokine expression, cells were stimulated for 5 h with phorbol 12-myristate 13-acetate (PMA; 200 nM) and ionomycin (1 µg/mL) in the presence of 10 µg/mL brefeldin A (all from Sigma-Aldrich) for the final 2.5 h of culture, followed by fixation and permeabilization. Cells were then stained with anti-cytokine antibodies (all from BioLegend) conjugated to different fluorochromes, and data were acquired using a Fortessa (BD Bioscience) cell analyzer. Flow cytometry data were analyzed with FlowJo. All flow cytometry and cell-sorting experiments adhered to recommended guidelines [57].

Cell lines and transfections. Jurkat T cells were cultured in RPMI-1640 medium supplemented with 1% glutamine, 1% non-essential amino acids, 1% sodium pyruvate, penicillin, streptomycin, kanamycin, 50 µM β-mercaptoethanol and 10% FBS. Jurkat cells were transiently transfected with the 100 µl Neon Transfection System kit (Thermo Fischer Scientific), using $3x10^6$ cells and 30 µg of plasmid DNA per condition and the following parameters: 1325 V, 10 ms, 3 pulses.

Plasmids. Expression plasmids encoding for the full-length human TET1, mouse Tet2 and human TET3 were obtained from Addgene (plasmids no. 49792, 41710 and 49446) [4, 29, 58]. The catalytically inactive form of mTet2, containing the amino acid substitutions H1302Y and D1304A, was generated by targeted mutagenesis using the QuickChange II XL Site-Directed Mutagenesis Kit (Agilent Technologies).

Quantitative RT-PCR. Total RNA was extracted using TRI reagent (MRC) and was reverse transcribed using the qScript cDNA SuperMix (Quanta Biosciences). Primer sequences for SYBR Green qRT-PCR are listed in the **Suppl. Table 1**. All qPCRs were performed with an ABI 7900HT Fast Real-Time PCR System (Applied Biosystems). Data were analyzed using the $2^{-\Delta\Delta Ct}$ method.

5hmC and 5mC measurements. For dot blot experiments, genomic DNA was isolated using the QIAamp DNA Micro Kit (Qiagen) and denatured with 1 M NaOH, 25 mM EDTA at 95°C for 10 min. Two-fold dilutions of the denatured DNA were then spotted on a nitrocellulose membrane, from a starting amount of 150-500 ng. Following nucleic acid crosslinking (80°C for 2 h), membranes were incubated with an anti-5hmC antibody (Active Motif) or an anti-5mC antibody (Epigentek), followed by incubation with an HRP-conjugated secondary antibody. Image acquisition was performed with the ImageQuant LAS 4000 (GE Healthcare Life Sciences), and quantification was performed using the Multi Gauge software. The number of pmol of 5hmC (or 5mC) per µg of genomic DNA in the different samples was calculated by comparing the intensity of the signal in the experimental sample with that of a standard with known concentration.

Methylated and hydroxymethylated DNA immunoprecipitation (MeDIP/hMeDIP) and qPCR. Genomic DNA from primary naïve and memory T lymphocytes was isolated using the DNeasy Blood & Tissue kit (Qiagen), after which 2.5 µg of DNA were sonicated (Bioruptor, Diagenode) to produce fragments ranging between 300 and 500 bp. MeDIP was performed using a MeDIP Kit (Zymo Research) following manufacturer's instruction. Briefly, 500 ng of sonicated DNA were denatured for 5 min at 98°C prior to incubation with 5 µg of anti-5mC antibody for 1 h at 37°C. For hMeDIP,

sonicated DNA was denatured for 10 min at 95°C, and 1 µg of denatured DNA was incubated overnight at 4°C with 1 µg of anti-5hmC rabbit antibody (Active Motif). For both MeDIP and hMeDIP, 500 ng of each sample of sonicated DNA were set aside as input. DNA-antibody complexes were immunoprecipitated for 3 h at 4°C with 20 µl of Dynabeads Protein G (Invitrogen). Magnetic beads were washed 5 times with 1x immunoprecipitation (IP) buffer (10x IP buffer: 100 mM Na-Phosphate pH 7.0, 1.4 M NaCl, 0.5 % Triton X- 100). Beads were then re-suspended in digestion buffer (50 mM Tris pH 8.0, 10 mM EDTA, 0.5 % SDS) containing 30 µg of Proteinase K (Ambion) and incubated for 3 h at 50°C. Finally, immunoprecipitated DNA was purified using the E.Z.N.A. Cycle Pure Kit (VWR-International AG). Quantitative PCR was performed with a 7900HT Fast Real Time PCR System (Applied Biosystems) and the percentage of immunoprecipitated hydroxymethylated or methylated DNA was calculated as follows: % input = $2^{(Ct\ input - Ct\ IP)}$ x input dilution factor x 100 [59]. *Controls for MeDIP and hMeDIP.* To optimize hMeDIP efficiency and as a quality control for each immunoprecipitation, a control DNA was produced by mixing 1:6 ratio of two otherwise identical PCR products containing either d5hmCTP or dCTP (1ng 5hmC-PCR : 6 ng C-PCR). Prior to IP, 2 ng of control DNA mix were spiked into every sample and after IP, PCR amplification was performed with primers specific for the control DNA. Because an EcoRV restriction site was present only in the 5hmC-PCR, further digestion with EcoRV was used to determine the specific enrichment of the 5hmC-containing product following IP. Similarly, to assess MeDIP efficiency, a control DNA mix containing 1:4 ratio of *in vitro* methylated and non-methylated pUC19 plasmids (MeDIP Kit, Zymo) was added to each sample prior IP. MeDIP efficiency was then evaluated by NcoI digestion exactly as described [59].

Reduced Representation Bisulfite Sequencing (RRBS). Primary naïve and memory T lymphocytes were obtained from two independent donors and were either left resting or were stimulated for 3 days with anti-CD3 and anti-CD28 antibodies. Genomic DNA was purified using the DNeasy Blood & Tissue Kit (Qiagen) and the RRBS experiment itself was outsourced to the Diagenode Premium RRBS technology service. The aligned (to the hg19 human reference genome) output data were processed using methylKit R package [60]. Briefly, Bismark outputs coverage2cytosine.txt reports were read by methRead() function. Bases with coverage below 10 reads, as well as the one displaying extremely high read coverage (>99.9th percentile of coverage in each sample), were filtered out. Samples in each group were pooled to obtain one representative methylation profile per sample group and differential methylated CpG dinucleotides were calculated through the calculateDiffMeth() function according to Fisher's exact test. To annotate differential methylated CpGs, only CpGs displaying at least 50% of changes in methylation level and having a q-value (false discovery rate corrected p-value from Fisher's exact test) ≤ 0.05 were retained. Annotation information was retrieved from a BED file containing gene annotation information based on hg19 alignment downloaded from UCSC Genome Browser. The RRBS data have been deposited in the Gene Expression Omnibus (GEO) database (accession no. GSE113884).

Analysis of hMeDIP-seq data. hMeDIP-seq data were obtained from Nestor *et al.* [27]. Antonio Lentini (Centre for Personalized Medicine, Linköping, Sweden) kindly provided alignments in *.bam format, which were visualized and analyzed with Integrative Genomics Viewer software (IGV). Early, late and housekeeping genes were defined in an unbiased manner, by analyzing gene expression raw data from Agilent 450k microarray from the same publication [27] using R software and Microsoft

Excel. To obtain the list of late genes, the following criteria were used: (i) differential expression (DE) in T_H1 cells between day 0 and day 1 of activation; (ii) DE in T_H1 cells between day 1 and day 5 of activation; (iii) Log_2 DE >1; (iv) increased expression between day 1 and day 5; (v) sum of expression values for raw data in all groups > 34. Housekeeping genes were defined as being (i) not differentially expressed between the various groups, and (ii) with a minimum expression above 6.7 in the naïve T cell group. Similarly, early genes were obtained as follows: (i) genes DE between day 1 and day 5 of activation; (ii) no DE between day 0 and day 1; (iii) Log_2DE > 1; (iv) decreased expression between day 1 and day 5; (v) sum of expression values for raw data in all groups > 34. Gene lists were then analyzed using DAVID [61, 62] and genes related to T cells and immunity gene ontology categories were selected. Finally, the 5hmC levels of the corresponding annotated enhancers for these genes were analyzed. Read counts of 5hmC for these enhancers were obtained with Samtools software for Linux. Analysis was performed on both the "BB" and "BC" set of samples from $CD4^+$ T cells *in vitro* polarized towards the T_H1 or T_H2 subsets. Graphs of read counts were made with GraphPad Prism 7. Enhancers and regulatory regions are indicated on the coverage plots either as GeneHancer Identifiers (GH) from FANTOM database or as CNSs (Conserved Noncoding Sequences). All references are according to the GRCh37/hg19 assembly.

Statistical analysis. Statistical analysis was performed with Prism software (GraphPad). Data are represented as mean ± SEM or SD, and significance was assessed by paired or unpaired Student's t test, two-tailed.

Author Contributions

LV and CL designed and performed experiments and analyzed data; MC and IK analyzed data; SM overviewed the project, analyzed data and wrote the manuscript with input from all authors.

Acknowledgements

The authors would like to thank David Jarossay and Jessica Marcandalli for invaluable technical support; Antonio Lentini for providing the alignment of published hMeDIP data; Margot Thome-Miazza, Nathalie Rufer, Greta Guarda and Daniel Speiser for helpful comments; Gioacchino Natoli for critical reading of the manuscript. This work was supported by the Swiss National Science Foundation (grant number 156875 and 175569 to SM).

Conflict of interest statement

The authors declare no financial or commercial conflict of interest.

References

1 **Smith, Z. D. and Meissner, A.,** DNA methylation: roles in mammalian development. *Nat Rev Genet* 2013. **14**: 204-220.

2 **Bird, A.,** DNA methylation patterns and epigenetic memory. *Genes Dev* 2002. **16**: 6-21.

3 **Wu, X. and Zhang, Y.,** TET-mediated active DNA demethylation: mechanism, function and beyond. *Nat Rev Genet* 2017. **18**: 517-534.

4 **Tahiliani, M., Koh, K. P., Shen, Y., Pastor, W. A., Bandukwala, H., Brudno, Y., Agarwal, S., Iyer, L. M., et al.,** Conversion of 5-methylcytosine to 5-hydroxymethylcytosine in mammalian DNA by MLL partner TET1. *Science* 2009. **324**: 930-935.

5 **Ito, S., D'Alessio, A. C., Taranova, O. V., Hong, K., Sowers, L. C. and Zhang, Y.,** Role of Tet proteins in 5mC to 5hmC conversion, ES-cell self-renewal and inner cell mass specification. *Nature* 2010. **466**: 1129-1133.

6 **Kriaucionis, S. and Heintz, N.,** The nuclear DNA base 5-hydroxymethylcytosine is present in Purkinje neurons and the brain. *Science* 2009. **324**: 929-930.

7 **Tsagaratou, A., Aijo, T., Lio, C. W., Yue, X., Huang, Y., Jacobsen, S. E., Lahdesmaki, H. and Rao, A.,** Dissecting the dynamic changes of 5-hydroxymethylcytosine in T-cell development and differentiation. *Proc Natl Acad Sci U S A* 2014. **111**: E3306-3315.

8 **Tsagaratou, A., Lio, C. J., Yue, X. and Rao, A.,** TET Methylcytosine Oxidases in T Cell and B Cell Development and Function. *Front Immunol* 2017. **8**: 220.

9 **Yu, M., Hon, G. C., Szulwach, K. E., Song, C. X., Zhang, L., Kim, A., Li, X., Dai, Q., et al.,** Base-resolution analysis of 5-hydroxymethylcytosine in the mammalian genome. *Cell* 2012. **149**: 1368-1380.

10 **Scott-Browne, J. P., Cw, L. and Rao, A.,** TET proteins in natural and induced differentiation. *Curr Opin Genet Dev* 2017. **46**: 202-208.

11 **Kanno, Y., Vahedi, G., Hirahara, K., Singleton, K. and O'Shea, J. J.,** Transcriptional and epigenetic control of T helper cell specification: molecular mechanisms underlying commitment and plasticity. *Annu Rev Immunol* 2012. **30**: 707-731.

12 **Bevington, S. L., Cauchy, P., Piper, J., Bertrand, E., Lalli, N., Jarvis, R. C., Gilding, L. N., Ott, S., et al.,** Inducible chromatin priming is associated with the establishment of immunological memory in T cells. *EMBO J* 2016. **35**: 515-535.

13 **Kersh, E. N., Fitzpatrick, D. R., Murali-Krishna, K., Shires, J., Speck, S. H., Boss, J. M. and Ahmed, R.,** Rapid demethylation of the IFN-gamma gene occurs in memory but not naive CD8 T cells. *J Immunol* 2006. **176**: 4083-4093.

14 **Makar, K. W. and Wilson, C. B.,** DNA methylation is a nonredundant repressor of the Th2 effector program. *J Immunol* 2004. **173**: 4402-4406.

15 **Makar, K. W., Perez-Melgosa, M., Shnyreva, M., Weaver, W. M., Fitzpatrick, D. R. and Wilson, C. B.,** Active recruitment of DNA methyltransferases regulates interleukin 4 in thymocytes and T cells. *Nat Immunol* 2003. **4**: 1183-1190.

16 **Bruniquel, D. and Schwartz, R. H.,** Selective, stable demethylation of the interleukin-2 gene enhances transcription by an active process. *Nat Immunol* 2003. **4**: 235-240.

17 **Gamper, C. J., Agoston, A. T., Nelson, W. G. and Powell, J. D.,** Identification of DNA methyltransferase 3a as a T cell receptor-induced regulator of Th1 and Th2 differentiation. *J Immunol* 2009. **183**: 2267-2276.

18 **Lee, P. P., Fitzpatrick, D. R., Beard, C., Jessup, H. K., Lehar, S., Makar, K. W., Perez-Melgosa, M., Sweetser, M. T., et al.,** A critical role for Dnmt1 and DNA methylation in T cell development, function, and survival. *Immunity* 2001. **15**: 763-774.

19 **Yu, Q., Zhou, B., Zhang, Y., Nguyen, E. T., Du, J., Glosson, N. L. and Kaplan, M. H.,** DNA methyltransferase 3a limits the expression of interleukin-13 in T helper 2 cells and allergic airway inflammation. *Proc Natl Acad Sci U S A* 2012. **109**: 541-546.

20 **Scharer, C. D., Barwick, B. G., Youngblood, B. A., Ahmed, R. and Boss, J. M.,** Global DNA methylation remodeling accompanies CD8 T cell effector function. *J Immunol* 2013. **191**: 3419-3429.

21 **Durek, P., Nordstrom, K., Gasparoni, G., Salhab, A., Kressler, C., de Almeida, M., Bassler, K., Ulas, T., et al.,** Epigenomic Profiling of Human CD4(+) T Cells Supports a Linear Differentiation Model and Highlights Molecular Regulators of Memory Development. *Immunity* 2016. **45**: 1148-1161.

22 **Komori, H. K., Hart, T., LaMere, S. A., Chew, P. V. and Salomon, D. R.,** Defining CD4 T cell memory by the epigenetic landscape of CpG DNA methylation. *J Immunol* 2015. **194**: 1565-1579.

23 **Hashimoto, S., Ogoshi, K., Sasaki, A., Abe, J., Qu, W., Nakatani, Y., Ahsan, B., Oshima, K., et al.,** Coordinated changes in DNA methylation in antigen-specific memory CD4 T cells. *J Immunol* 2013. **190**: 4076-4091.

24 **Bird, J. J., Brown, D. R., Mullen, A. C., Moskowitz, N. H., Mahowald, M. A., Sider, J. R., Gajewski, T. F., Wang, C. R., et al.,** Helper T cell differentiation is controlled by the cell cycle. *Immunity* 1998. **9**: 229-237.

25 **Ko, M., Bandukwala, H. S., An, J., Lamperti, E. D., Thompson, E. C., Hastie, R., Tsangaratou, A., Rajewsky, K., et al.,** Ten-Eleven-Translocation 2 (TET2) negatively regulates homeostasis and differentiation of hematopoietic stem cells in mice. *Proc Natl Acad Sci U S A* 2011. **108**: 14566-14571.

26 **Ichiyama, K., Chen, T., Wang, X., Yan, X., Kim, B. S., Tanaka, S., Ndiaye-Lobry, D., Deng, Y., et al.,** The methylcytosine dioxygenase Tet2 promotes DNA demethylation and activation of cytokine gene expression in T cells. *Immunity* 2015. **42**: 613-626.

27 **Nestor, C. E., Lentini, A., Hagg Nilsson, C., Gawel, D. R., Gustafsson, M., Mattson, L., Wang, H., Rundquist, O., et al.,** 5-Hydroxymethylcytosine Remodeling Precedes Lineage Specification during Differentiation of Human CD4(+) T Cells. *Cell Rep* 2016. **16**: 559-570.

28 **Jin, C., Lu, Y., Jelinek, J., Liang, S., Estecio, M. R., Barton, M. C. and Issa, J. P.,** TET1 is a maintenance DNA demethylase that prevents methylation spreading in differentiated cells. *Nucleic Acids Res* 2014. **42**: 6956-6971.

29 **Ko, M., Huang, Y., Jankowska, A. M., Pape, U. J., Tahiliani, M., Bandukwala, H. S., An, J., Lamperti, E. D., et al.,** Impaired hydroxylation of 5-methylcytosine in myeloid cancers with mutant TET2. *Nature* 2010. **468**: 839-843.

30 **Montagner, S., Leoni, C., Emming, S., Della Chiara, G., Balestrieri, C., Barozzi, I., Piccolo, V., Togher, S., et al.,** TET2 Regulates Mast Cell Differentiation and Proliferation through Catalytic and Non-catalytic Activities. *Cell Rep* 2016. **15**: 1566-1579.

31 **Blaschke, K., Ebata, K. T., Karimi, M. M., Zepeda-Martinez, J. A., Goyal, P., Mahapatra, S., Tam, A., Laird, D. J., et al.,** Vitamin C induces Tet-dependent DNA demethylation and a blastocyst-like state in ES cells. *Nature* 2013. **500**: 222-226.

32 **Yin, R., Mao, S. Q., Zhao, B., Chong, Z., Yang, Y., Zhao, C., Zhang, D., Huang, H., et al.,** Ascorbic acid enhances Tet-mediated 5-methylcytosine oxidation and promotes DNA demethylation in mammals. *J Am Chem Soc* 2013. **135**: 10396-10403.

33 **Yue, X., Trifari, S., Aijo, T., Tsagaratou, A., Pastor, W. A., Zepeda-Martinez, J. A., Lio, C. W., Li, X., et al.,** Control of Foxp3 stability through modulation of TET activity. *J Exp Med* 2016. **213**: 377-397.

34 **Geginat, J., Sallusto, F. and Lanzavecchia, A.,** Cytokine-driven proliferation and differentiation of human naive, central memory, and effector memory CD4(+) T cells. *J Exp Med* 2001. **194**: 1711-1719.

35 **Unutmaz, D., Pileri, P. and Abrignani, S.,** Antigen-independent activation of naive and memory resting T cells by a cytokine combination. *J Exp Med* 1994. **180**: 1159-1164.

36 **Geginat, J., Lanzavecchia, A. and Sallusto, F.,** Proliferation and differentiation potential of human CD8+ memory T-cell subsets in response to antigen or homeostatic cytokines. *Blood* 2003. **101**: 4260-4266.

37 **Bock, C., Tomazou, E. M., Brinkman, A. B., Muller, F., Simmer, F., Gu, H., Jager, N., Gnirke, A., et al.,** Quantitative comparison of genome-wide DNA methylation mapping technologies. *Nat Biotechnol* 2010. **28**: 1106-1114.

38 **Meissner, A., Mikkelsen, T. S., Gu, H., Wernig, M., Hanna, J., Sivachenko, A., Zhang, X., Bernstein, B. E., et al.,** Genome-scale DNA methylation maps of pluripotent and differentiated cells. *Nature* 2008. **454**: 766-770.

39 **Chen, E. Y., Tan, C. M., Kou, Y., Duan, Q., Wang, Z., Meirelles, G. V., Clark, N. R. and Ma'ayan, A.,** Enrichr: interactive and collaborative HTML5 gene list enrichment analysis tool. *BMC Bioinformatics* 2013. **14**: 128.

40 **Grogan, J. L., Mohrs, M., Harmon, B., Lacy, D. A., Sedat, J. W. and Locksley, R. M.,** Early transcription and silencing of cytokine genes underlie polarization of T helper cell subsets. *Immunity* 2001. **14**: 205-215.

41 **Schoenborn, J. R., Dorschner, M. O., Sekimata, M., Santer, D. M., Shnyreva, M., Fitzpatrick, D. R., Stamatoyannopoulos, J. A. and Wilson, C. B.,** Comprehensive epigenetic profiling identifies multiple distal regulatory elements directing transcription of the gene encoding interferon-gamma. *Nat Immunol* 2007. **8**: 732-742.

42 **Mumbach, M. R., Satpathy, A. T., Boyle, E. A., Dai, C., Gowen, B. G., Cho, S. W., Nguyen, M. L., Rubin, A. J., et al.,** Enhancer connectome in primary human cells identifies target genes of disease-associated DNA elements. *Nat Genet* 2017. **49**: 1602-1612.

43 **Stadler, M. B., Murr, R., Burger, L., Ivanek, R., Lienert, F., Scholer, A., van Nimwegen, E., Wirbelauer, C., et al.,** DNA-binding factors shape the mouse methylome at distal regulatory regions. *Nature* 2011. **480**: 490-495.

44 **Calo, E. and Wysocka, J.,** Modification of enhancer chromatin: what, how, and why? *Mol Cell* 2013. **49**: 825-837.

45 **Verma, N., Pan, H., Dore, L. C., Shukla, A., Li, Q. V., Pelham-Webb, B., Teijeiro, V., Gonzalez, F., et al.,** TET proteins safeguard bivalent promoters from de novo methylation in human embryonic stem cells. *Nat Genet* 2018. **50**: 83-95.

46 **Manzo, M., Wirz, J., Ambrosi, C., Villasenor, R., Roschitzki, B. and Baubec, T.,** Isoform-specific localization of DNMT3A regulates DNA methylation fidelity at bivalent CpG islands. *EMBO J* 2017. **36**: 3421-3434.

47 **Hill, P. W. S., Leitch, H. G., Requena, C. E., Sun, Z., Amouroux, R., Roman-Trufero, M., Borkowska, M., Terragni, J., et al.,** Epigenetic reprogramming enables the transition from primordial germ cell to gonocyte. *Nature* 2018. **555**: 392-396.

48 **den Braber, I., Mugwagwa, T., Vrisekoop, N., Westera, L., Mogling, R., de Boer, A. B., Willems, N., Schrijver, et al.,** Maintenance of peripheral naive T cells is sustained by thymus output in mice but not humans. *Immunity* 2012. **36**: 288-297.

49 **Thome, J. J., Grinshpun, B., Kumar, B. V., Kubota, M., Ohmura, Y., Lerner, H., Sempowski, G. D., Shen, Y., et al.,** Longterm maintenance of human naive T cells through in situ homeostasis in lymphoid tissue sites. *Sci Immunol* 2016. **1**.

50 **Kumar, B. V., Connors, T. J. and Farber, D. L.,** Human T Cell Development, Localization, and Function throughout Life. *Immunity* 2018. **48**: 202-213.

51 **Vrisekoop, N., den Braber, I., de Boer, A. B., Ruiter, A. F., Ackermans, M. T., van der Crabben, S. N., Schrijver, E. H., Spierenburg, G., et al.,** Sparse production but preferential incorporation of recently produced naive T cells in the human peripheral pool. *Proc Natl Acad Sci U S A* 2008. **105**: 6115-6120.

52 **van den Broek, T., Borghans, J. A. M. and van Wijk, F.,** The full spectrum of human naive T cells. *Nat Rev Immunol* 2018.

53 **Lister, R., Mukamel, E. A., Nery, J. R., Urich, M., Puddifoot, C. A., Johnson, N. D., Lucero, J., Huang, Y., et al.,** Global epigenomic reconfiguration during mammalian brain development. *Science* 2013. **341**: 1237905.

54 **Wilson, C. B., Rowell, E. and Sekimata, M.,** Epigenetic control of T-helper-cell differentiation. *Nat Rev Immunol* 2009. **9**: 91-105.

55 **Rothenberg, E. V. and Zhang, J. A.,** T-cell identity and epigenetic memory. *Curr Top Microbiol Immunol* 2012. **356**: 117-143.

56 **Avni, O., Lee, D., Macian, F., Szabo, S. J., Glimcher, L. H. and Rao, A.,** T(H) cell differentiation is accompanied by dynamic changes in histone acetylation of cytokine genes. *Nat Immunol* 2002. **3**: 643-651.

57 **Cossarizza, A., Chang, H. D., Radbruch, A., Akdis, M., Andra, I., Annunziato, F., Bacher, P., Barnaba, V., et al.,** Guidelines for the use of flow cytometry and cell sorting in immunological studies. *Eur J Immunol* 2017. **47**: 1584-1797.

58 **Ko, M., An, J., Bandukwala, H. S., Chavez, L., Aijo, T., Pastor, W. A., Segal, M. F., Li, H., et al.,** Modulation of TET2 expression and 5-methylcytosine oxidation by the CXXC domain protein IDAX. *Nature* 2013. **497**: 122-126.

59 **Leoni, C., Montagner, S., Rinaldi, A., Bertoni, F., Polletti, S., Balestrieri, C. and Monticelli, S.,** Dnmt3a restrains mast cell inflammatory responses. *Proc Natl Acad Sci U S A* 2017. **114**: E1490-E1499.

60 **Akalin, A., Kormaksson, M., Li, S., Garrett-Bakelman, F. E., Figueroa, M. E., Melnick, A. and Mason, C. E.,** methylKit: a comprehensive R package for the analysis of genome-wide DNA methylation profiles. *Genome Biol* 2012. **13**: R87.

61 **Huang da, W., Sherman, B. T. and Lempicki, R. A.,** Systematic and integrative analysis of large gene lists using DAVID bioinformatics resources. *Nat Protoc* 2009. **4**: 44-57.

62 **Huang da, W., Sherman, B. T. and Lempicki, R. A.,** Bioinformatics enrichment tools: paths toward the comprehensive functional analysis of large gene lists. *Nucleic Acids Res* 2009. **37**: 1-13.

Figure Legends

Figure 1. Dynamics of 5mC and 5hmC changes in primary human T lymphocytes. (a) Freshly isolated naïve and **(b)** memory $CD4^+$ T lymphocytes were either left resting or were stimulated for five days with plate-bound anti-CD3 and anti-CD28 antibodies, followed by genomic DNA extraction and measurement of the levels of 5mC and **(c-d)** 5hmC by dot blot. Each dot represents one individual human donor and one independent experiment (at least n=6 experiments). **(e-f)** Ratio between genomic 5hmC and 5mC measured in the previous panels. Each dot represents one individual human donor and one independent experiment (at least n=6 experiments). Data are shown as mean ± SD. Unpaired t-test.

Figure 2. Loss of genomic 5hmC is a general feature of T cell activation. (a) Primary human naïve and memory $CD8^+$ T lymphocytes were either left resting or were stimulated for three and five days with plate-bound anti-CD3 and anti-CD28 antibodies, followed by measurement of the levels of genomic 5hmC (n=1). **(b)** Naïve $CD4^+$ and **(c**) $CD8^+$ murine spleen T lymphocytes were either left resting or were stimulated for three days with plate-bound anti-CD3 and anti-CD28 antibodies, followed by genomic DNA extraction and measurement of the levels of 5hmC. Each dot represents one mouse (n=3 biological samples) analyzed together in one experiment. Mean ± SD. Paired t-test. **(d)** Human naïve, central memory (T_{CM}) and effector memory (T_{EM}) T lymphocytes were isolated from peripheral blood and global levels of 5hmC were measured by dot blot. One representative blot is shown on the left, while the compiled analysis of several donors is shown on the right. Each dot represents one individual donor and one independent experiment (n=6 experiments). Mean ± SD. Paired t-test. **(e)** Individual effector subsets (T_H1, T_H2 and T_H17) were freshly isolated from peripheral blood and global levels of 5hmC were measured by dot blot. Each dot represents one individual donor and one independent experiment (n=2 experiments). Data are shown as mean ± SD.

Figure 3. DNA demethylation-related processes augment expression of effector cytokines. (a) Naïve and memory T cells were separated from peripheral blood and either left untreated or were stimulated for five days with plate-bound anti-CD3 and anti-CD28 antibodies, with or without addition of decitabine (1 μM or 5 μM). Genomic DNA was purified and global levels of 5mC were measured by dot blot (representative of n=3 experiments). **(b)** Same as (a), n=3 independent experiments. Mean ± SD. **(c)** Cells were treated as in (a), except that the expression of the indicated cytokines was measured by intracellular staining. Each dot represents one independent experiment (n=4 for IL-2 and IFN-γ and n=3 for IL-22). Mean ± SD. Paired t-test. **(d)** Jurkat T cells were transiently transfected with plasmids expressing either full-length mouse Tet2 (wild-type or mutated in the catalytic domain), human TET1 or human TET3. 48 h after transfection, genomic DNA was isolated and levels of 5hmC were measured by dot blot. Shown is one representative blot of at least n=3 independent experiments. **(e)** Cells were treated as in (d), except that they were also stimulated with PMA and ionomycin for 3 h to induce cytokine transcription, and total RNA was isolated. The expression of the indicated cytokines was measured by qRT-PCR, relative to UBE2D2 (Ubiquitin-conjugating enzyme E2 D2), used as endogenous control, and relative to cells transfected with an empty vector. Each dot represents one independent experiment (n=at least 3). Mean ± SEM. Unpaired t-test. **(f)** Naïve and memory T cells were stimulated for three days in the presence or absence of the

indicated concentrations of vitamin C. Levels of genomic 5hmC were measured by dot blot. Compiled results of n=3 independent experiments are shown on the right. Mean ± SD. Paired t-test, compared to untreated cells. **(g)** Cells were treated exactly as in (f), except that the expression of the indicated cytokines was measured by intracellular staining. Shown are the results obtained from cells treated with 100 μg/ ml vitamin C. Each dot represents one individual donor and one independent experiment (n=11). Data are shown as mean ± SD. Paired t-test.

Figure 4. TCR engagement is not strictly required for the loss of 5hmC in proliferating T cells. (a) Human naïve, T_{CM} and T_{EM} $CD4^+$ T cells were isolated from peripheral blood, loaded with the cell tracer CFSE to assess proliferation, and cultured in the presence of IL-2, IL-6 and TNF-α. Proliferation was measured after three and six days of culture (representative of n=3 independent experiments). Data were collected with a BD Fortessa and analyzed with FlowJo software. **(b)** Genomic DNA was purified from cells as in (a), and levels of 5hmC were measured by dot blot. One representative blot of n=3 independent experiments is shown. **(c)** Same as in (b); compiled results of n=3 independent experiments. Mean ± SD. **(d)** Human naïve and memory $CD8^+$ T cells were isolated from peripheral blood and treated as in (a), except that they were cultured in presence of IL-7 and IL-15 (representative of n=2 donors in two independent experiments). Data were collected with a BD Fortessa and analyzed with FlowJo software. **(e)** Dot blot to measure genomic 5hmC of cells treated as in (d) (representative of n=2 donors in two independent experiments).

Figure 5. Active DNA demethylation in naïve, but not memory T lymphocytes. (a) Naïve and memory T cells were stimulated with plate-bound anti-CD3 and anti-CD28 antibodies for the indicated times. The surface expression of early activation markers (CD25-PE, CD69-PE-Cy5) was determined at each time point by flow cytometry staining (representative of at least n=3 independent experiments). Data were collected with a BD Fortessa and analyzed with FlowJo software. **(b)** Same as (a), except that cells were loaded with CFSE prior to stimulation to measure the extent of cell proliferation at each time point (representative of at least n=3 independent experiments). **(c)** Same as (a), except that genomic DNA was extracted at the indicated time points, and levels of 5hmC were measured by dot blot (representative of at least n=3 independent experiments). **(d)** Compiled results of individual experiments performed as in (c). Each dot represents one donor and one independent experiment (at least n=3). Mean ± SD. Paired t-test, compared to unstimulated cells. **(e)** Cells were loaded with CFSE, followed by stimulation with plate-bound anti-CD3 and anti-CD28 antibodies. After 3 days, each indicated peak was sorted, and levels of 5hmC were measured by dot blot in comparison to unstimulated cells. Shown are the results of n=4 independent experiments. Data are shown as mean ± SD and were collected with a BD Fortessa and analyzed with FlowJo software.

Figure 6. Inhibition of cell division reduces the loss of 5hmC. (a) Naïve and memory T lymphocytes were loaded with CFSE and activated for three days with anti-CD3 and anti-CD28 antibodies in the presence or absence of the cell cycle inhibitors aphidicolin and nocodazole. The extent of cell proliferation was determined by CSFE dilution, while cell activation was evaluated by measuring cell size (FSC) and surface expression of CD25. Shown is one representative result for

naïve T cells (n=5 independent experiments). Data were collected with a BD Fortessa and analyzed with FlowJo software. **(b)** Cells were treated as in (a), and levels of 5hmC in the genomic DNA were measured by dot blot (independent experiments: n=5 for naïve T cells and n=4 for memory T cells). **(c)** Compiled results of individual experiments performed as in (b). Each dot represents one donor and one independent experiment (n=5 for naïve T cells and n=4 for memory T cells). Data are shown as mean ± SD. Paired t-test, compared to unstimulated cells.

Figure 7. Dynamic changes of 5mC and 5hmC at regulatory regions of immune-related genes. **(a)** Left: volcano plot showing the differentially methylated regions observed by RRBS between freshly isolated naïve and memory T lymphocytes (n=2 independent donors analyzed in one RRBS experiment). Right: the differentially methylated regions shown in (a) were analyzed for their genomic location. **(b)** Selected GO terms significantly associated with hypo- or hyper-methylated promoter regions are shown. Differentially methylated regions located in the region upstream of the TSS (0 to -1500bp), with q-value ≤0.2 and with a methylation difference of at least 33% were selected for the analysis, which was performed using EnrichR [39]. **(c)** Levels of 5hmC in differentiated T cells at the indicated loci as assessed by hMeDIP-seq [27]. **(d)** MeDIP (top) or hMeDIP (bottom) experiments were performed on naïve and memory T cells either resting or stimulated for 5 days with plate-bound anti-CD3 and anti-CD28 antibodies. The enrichment for the indicated regulatory regions was measured by qPCR. Each dot represents one donor and one independent experiment (n≥3). Mean ± SD. Paired t-test. **(e)** Correlation of 5hmC signal with ATAC-accessible regions in a window of 10 kb in human naïve T lymphocytes. A score matrix of 5hmC score around ATAC peak positions was built starting from available data [27, 42].

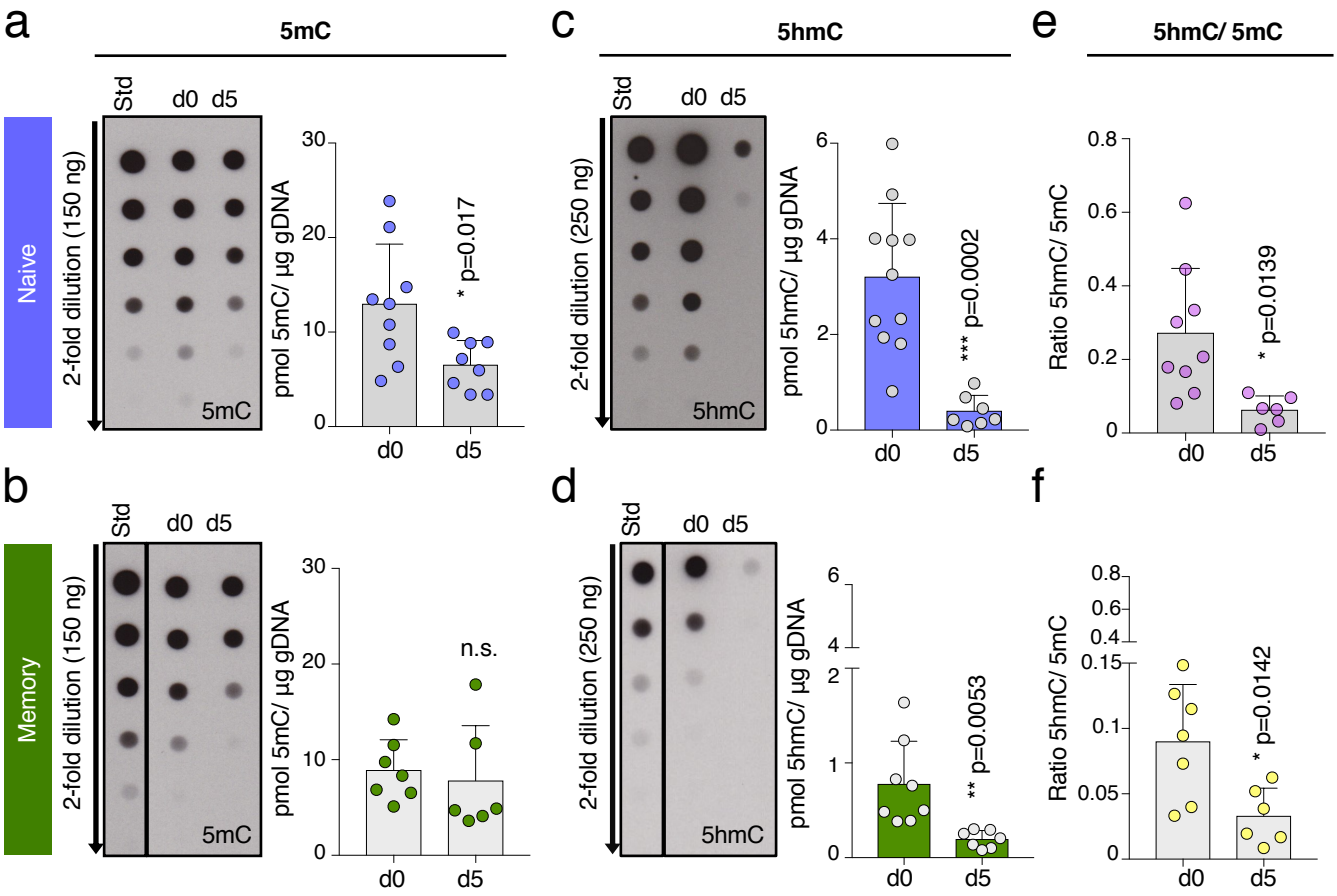

Vincenzetti – Figure 1

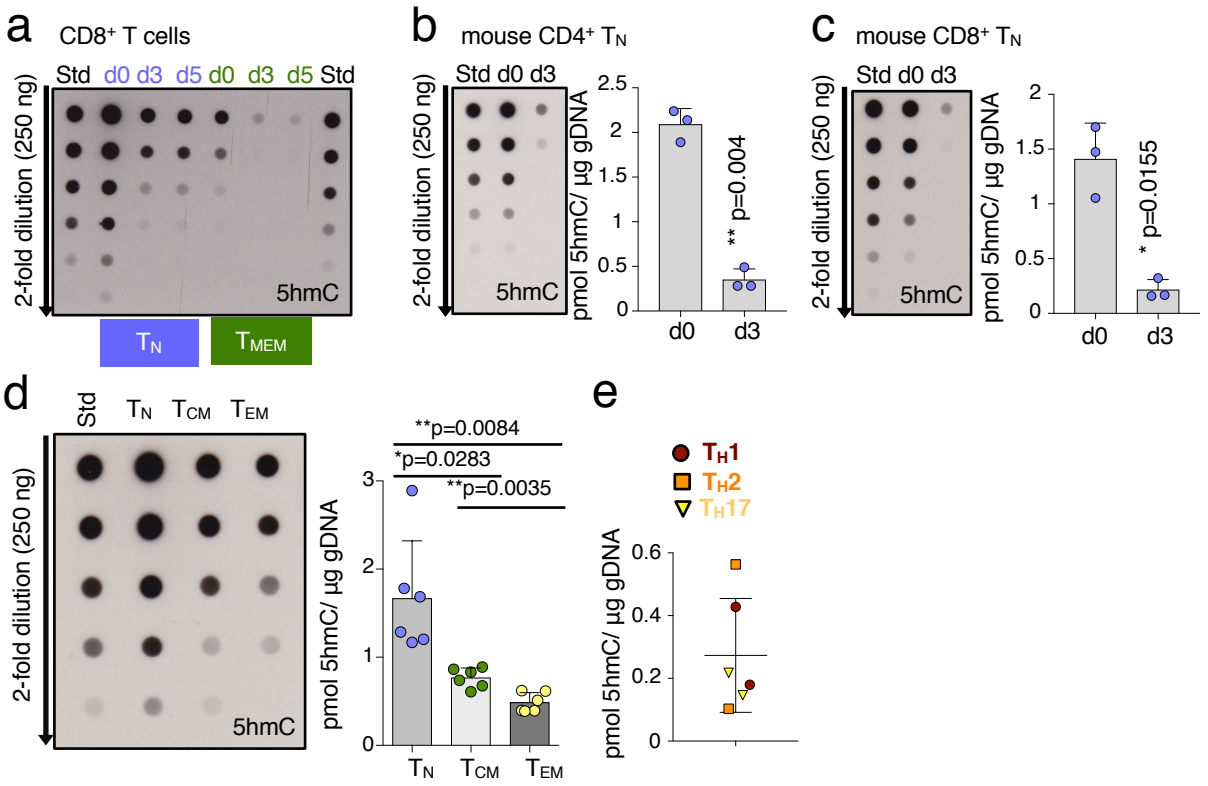

Vincenzetti – Figure 2

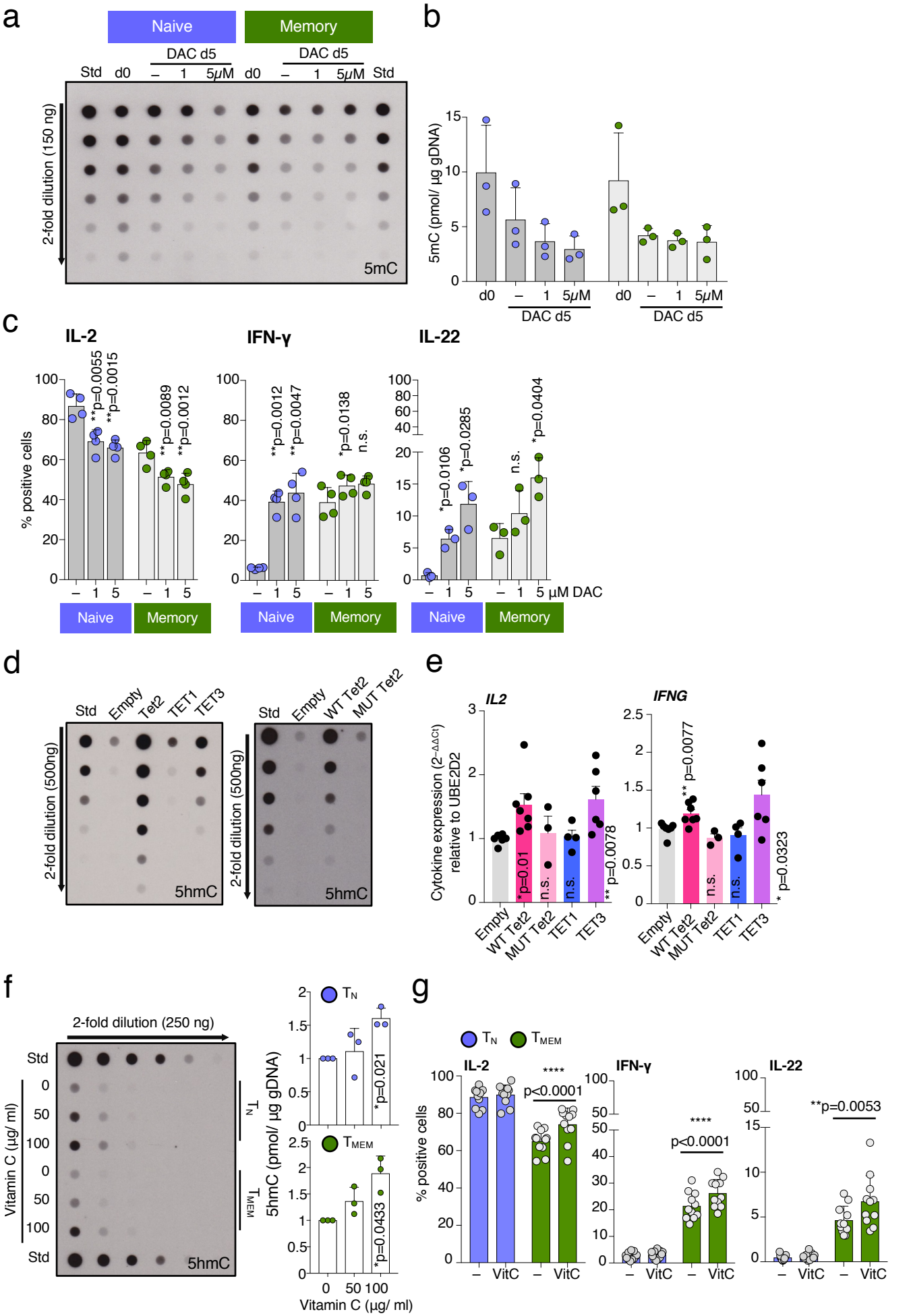

Vincenzetti – Figure 3

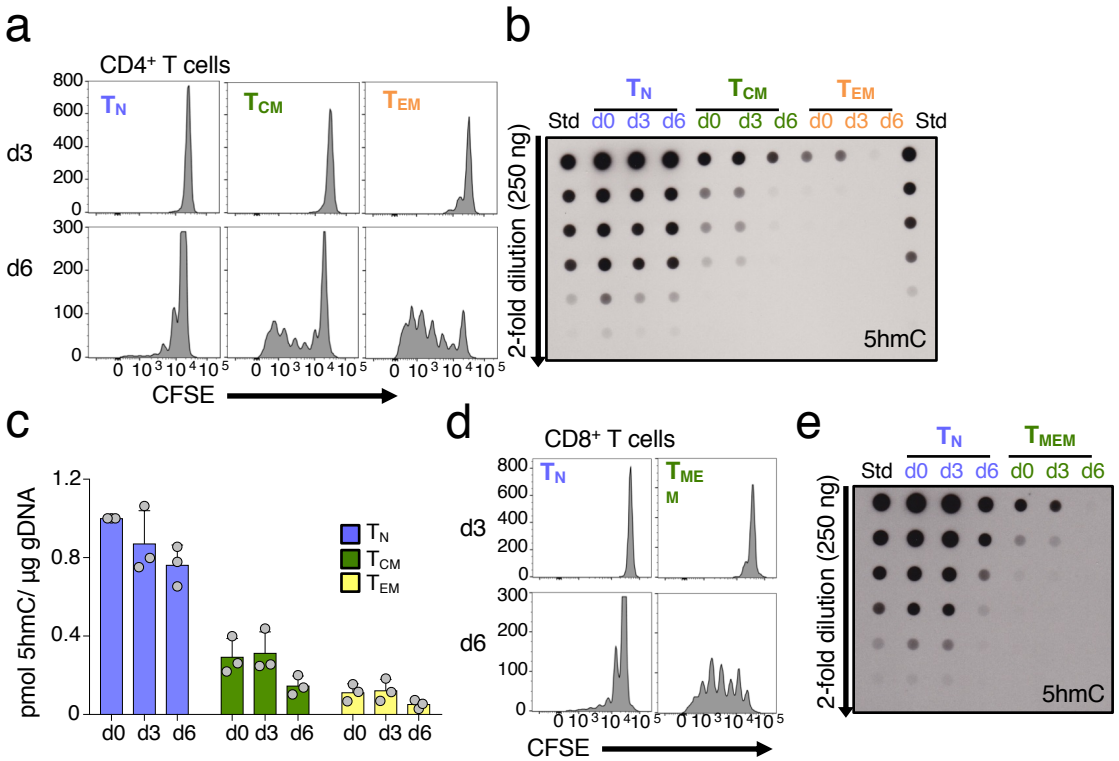

Vincenzetti – Figure 4

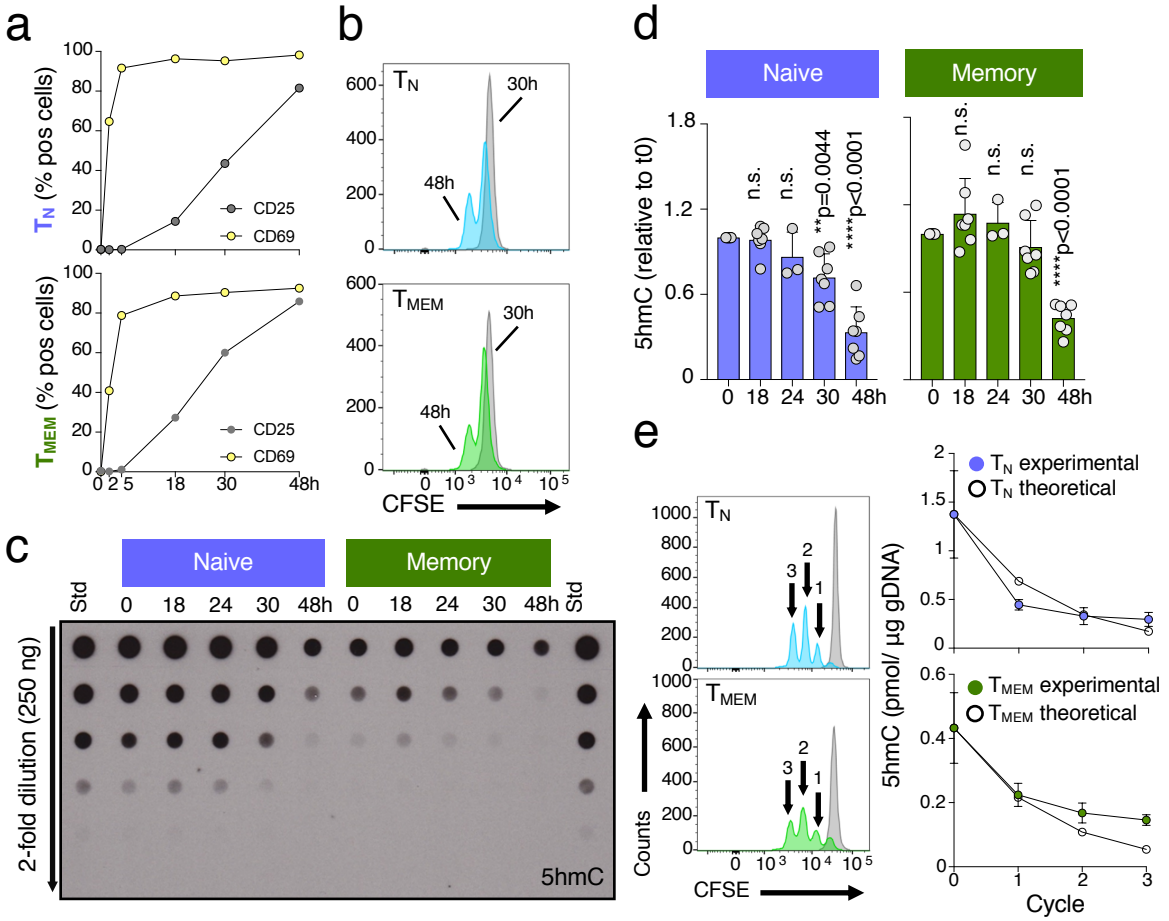

Vincenzetti – Figure 5

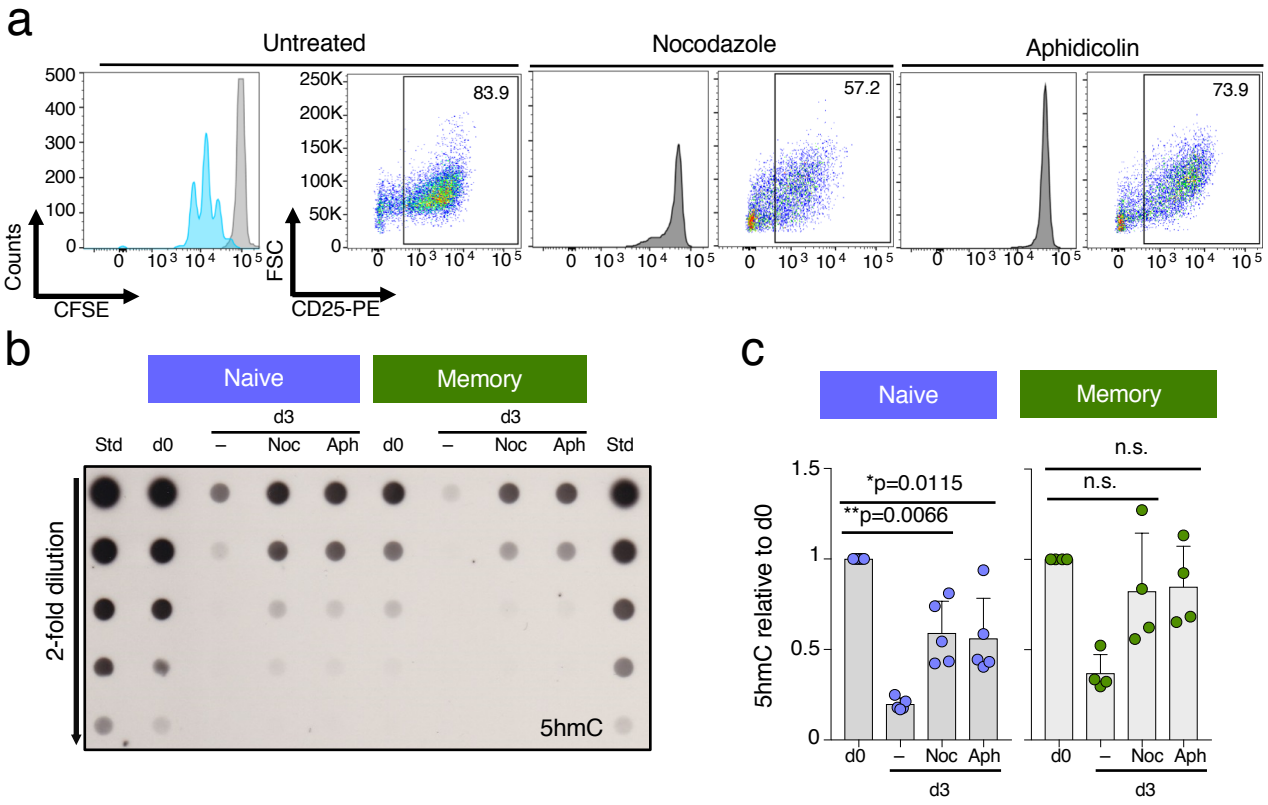

Vincenzetti – Figure 6

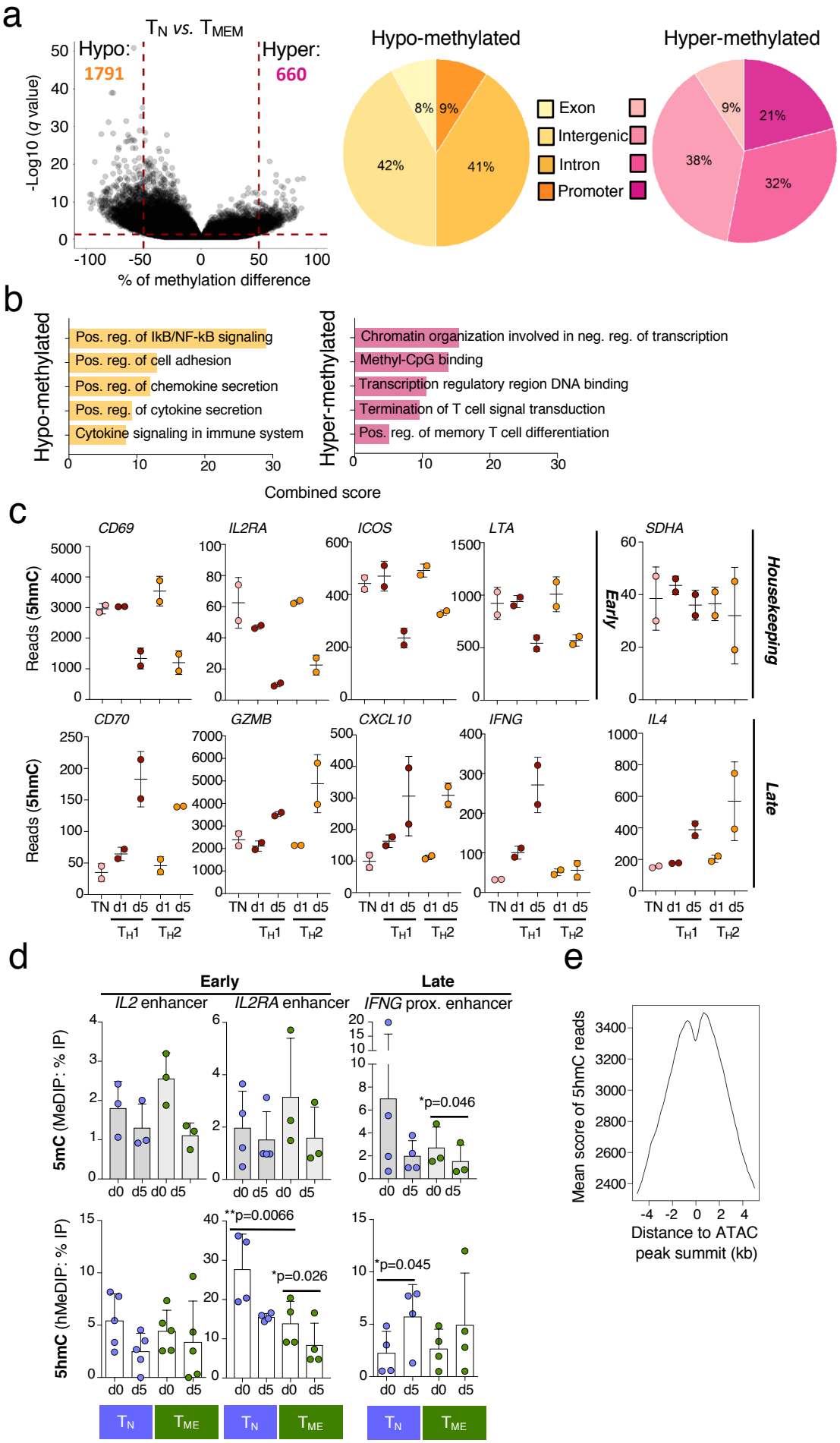

Vincenzetti – Figure 7